Published in final edited form as:

Cell Rep. 2021 July 13; 36(2): 109382. doi:10.1016/j.celrep.2021.109382.

In vivo dynamic 3D imaging of oocytes and embryos in the mouse oviduct

Shang Wang[1,*], **Irina V. Larina**[2,3,*]

[1]Department of Biomedical Engineering, Stevens Institute of Technology, Hoboken, NJ 07030, USA

[2]Department of Molecular Physiology and Biophysics, Baylor College of Medicine, Houston, TX 77030, USA

[3]Lead contact

SUMMARY

Developmental biologists have always relied on imaging to shed light on dynamic cellular events. However, processes such as mammalian fertilization and embryogenesis are generally inaccessible for direct imaging. In consequence, how the oviduct (fallopian tube) facilitates the transport of gametes and preimplantation embryos continues to be unanswered. Here we present a combination of intravital window and optical coherence tomography for dynamic, volumetric, *in vivo* imaging of oocytes and embryos as they are transported through the mouse oviduct. We observed location-dependent circling, oscillating, and long-distance bi-directional movements of oocytes and embryos that suggest regulatory mechanisms driving transport and question established views in the field. This *in vivo* imaging approach can be combined with a variety of genetic and pharmacological manipulations for live functional analysis, bringing the potential to investigate reproductive physiology in its native state.

Graphical abstract

*Correspondence: shang.wang@stevens.edu (S.W.), larina@bcm.edu (I.V.L.).

AUTHOR CONTRIBUTIONS

Conceptualization, S.W. and I.V.L.; methodology, S.W. and I.V.L.; investigation, S.W. and I.V.L.; writing – original draft, S.W.; writing – review & editing, S.W. and I.V.L.; funding acquisition, S.W. and I.V.L.

SUPPLEMENTAL INFORMATION

Supplemental information can be found online at https://doi.org/10.1016/j.celrep.2021.109382.

DECLARATION OF INTERESTS

The authors declare no competing interests.

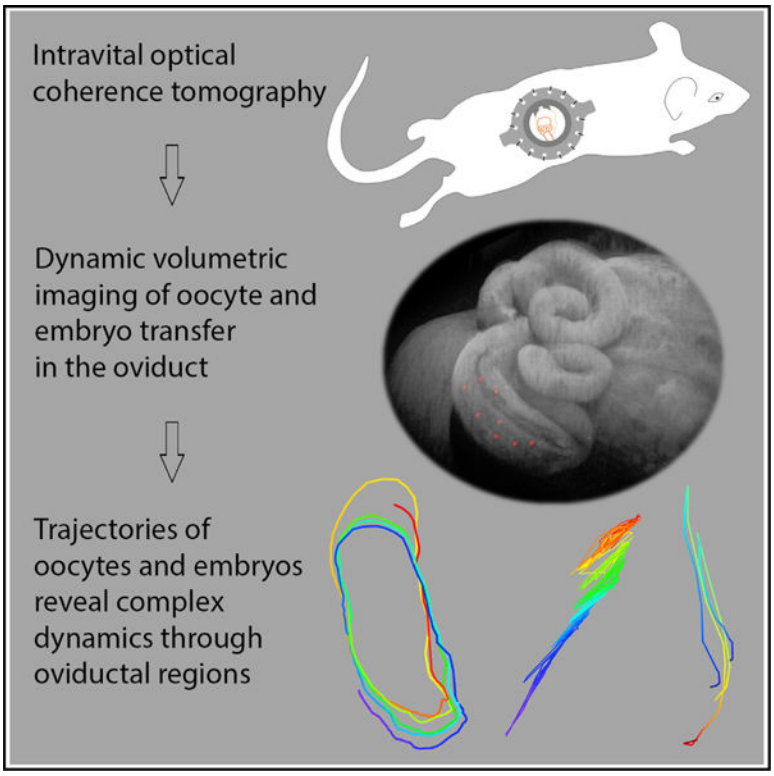

In brief

Wang and Larina present *in vivo* volumetric imaging of oocytes and embryos as they are transported through the mouse oviduct with optical coherence tomography and an intravital microscopy. The study reveals complex dynamics of oocytes and embryos that suggest a regulatory role of cilia and oviductal contractions in driving the transport.

INTRODUCTION

The mammalian oviduct (fallopian tube) is a tubular organ connecting the ovary and the uterus. Largely because of the success of assisted reproductive technologies (ARTs), which bypass the oviduct to achieve pregnancy (Ménézo et al., 2015), research on the oviduct has been somewhat neglected, and its physiology is less understood as compared with other female reproductive organs. However, despite continuous advancements, ART still suffers from a low efficacy that is far from comparable with natural pregnancy (Avilés et al., 2015; Besenfelder et al., 2012). This issue has recently led to the consensus that a better understanding of the oviductal physiology and function is essential for further optimization of ART by *in vitro* simulation of the *in vivo* conditions during the oviductal transport (Li and Winuthayanon, 2017). In addition, oviductal dysfunction is thought to be associated with reproductive disorders, including tubal ectopic pregnancy, whose etiology remains largely unknown (Shaw et al., 2010). Elucidating the functional roles of the oviduct is therefore significant to unravel the mechanisms underlying such reproductive disorders, which could contribute to strategies of prevention and early diagnosis.

The oviduct delivers gametes toward fertilization, transfers embryos to the uterus in a precise temporal manner, and provides the environment for successful fertilization and preimplantation development (Coy et al., 2012). The transport of gametes and embryos is believed to be facilitated by the oviductal motile cilia, smooth muscle, and secretory flows (Ezzati et al., 2014). Although little is known regarding the individual roles of these factors (Besenfelder et al., 2012; Coy et al., 2012; Li and Winuthayanon, 2017), it is generally accepted that the oviductal cilia are the primary driver of oocytes/embryos toward the uterus for implantation (Coy et al., 2012; Halbert et al., 1976a; Lyons et al., 2006; Spassky and Meunier, 2017). To determine the requirement of these activities for the oviductal transport, targeted inhibitions have been implemented, but analysis has mainly relied on evaluating the final outcome, such as whether oocytes reach the fertilization site or whether embryos are implanted (Halbert et al., 1976a, 1989; Horne et al., 2008). The detailed dynamics of the oocyte/embryo transport preceding fertilization and implantation remain unclear for both normal and disrupted conditions. This gap in knowledge is largely due to a lack of imaging techniques capable of visualizing mammalian intra-oviductal events *in vivo*. The oviduct exhibits a complex biochemical and biomechanical luminal environment that has spatiotemporal variations and responds to a number of internal and external stimulations, such as hormones and sperm (Buhi et al., 1997; Fauci and Dillon, 2006; Georgiou et al., 2005, 2007; Menezo and Guerin, 1997). This complexity makes the oviduct difficult to fully model *in vitro* or *ex vivo.* Because much of our understanding of oocyte/embryo dynamics is largely derived from extrapolation of such systems, the reproductive community has called for *in vivo* verification of current models (Avilés et al., 2015; Coy et al., 2012; Ménézo et al., 2015). This goal requires the development of new imaging technologies.

In vivo imaging of the oviduct has been pursued in a number of studies (Battalia and Yanagimachi, 1979; Bochner et al., 2015; Hino and Yanagimachi, 2019; Ishikawa et al., 2016; Muro et al., 2016; Wang and Larina, 2018b; Wang et al., 2018), with a primary focus on understanding sperm transport and oviductal fluid flows. Recently, with the externalized ovary, oviduct, and upper uterus well kept under physiological conditions, Hino and Yanagimachi (2019) highlighted the role of directional oviductal fluid flows in sperm movement and fertilization. However, resolving and tracking oocytes and embryos in 3D through the oviductal wall, with sufficient volume rate and field of view, is technically challenging and cannot be accomplished by widely used high-resolution techniques, such as bright-field, epifluorescence, and confocal microscopy. To address this technical limitation, we have developed an approach for volumetric *in vivo* imaging of the mouse oviduct using optical coherence tomography (OCT). OCT is a label-free modality employing low-coherence interferometry for depth-resolved imaging (Huang et al., 1991). A single unit of OCT data is an in-depth line, called an A-scan; lateral scanning of the imaging beam produces 2D images (B-scans), and 2D scanning produces volumetric imaging. Its micro-scale resolution and millimeter-level imaging depth in scattering tissues provide an ideal imaging scale for the mouse oviduct (Burton et al., 2015). To bypass the skin and muscle layers, we implemented an intravital imaging approach, which involves implantation of a 3D-printed imaging window on the dorsal side of a mouse for access to the oviduct. We previously showed that OCT can reveal structural details of the oviduct *in vivo* at a ~5-μm resolution (Burton et al., 2015; Wang et al., 2018) and also established functional OCT

methods for mapping the cilia beat frequency and tracking spermatozoa *in vivo* (Wang et al., 2015a; Wang and Larina, 2018b). However, 3D imaging of the dynamics of oocytes and embryos during their journey through the oviduct has not been demonstrated before.

Here, we report *in vivo* volumetric OCT imaging and tracking of oocytes and preimplantation embryos within the native environment of the mouse oviduct. We present 4D (3D + time) visualizations through different sections of the oviduct, revealing a variety of unexpected movement patterns as oocytes and embryos transit from the upper ampulla to the lower isthmus. The spatially dependent dynamics of oocytes and embryos in the oviduct indicate movements that were not known before, suggesting that the mechanisms of the oviductal transport are more complex than previously thought. This *in vivo* imaging approach sets a platform for future studies investigating the mammalian reproduction from a dynamic perspective, providing insights into the process of oviductal transport in its native state, and leading to a more complete understanding of reproductive pathologies.

Design

In vivo dynamic visualization of oocytes and embryos in the mouse oviduct requires a combination of animal manipulation approach providing *in vivo* access to the reproductive organs and an imaging modality with sufficient resolution and imaging depth to capture these dynamics. In our early attempts to access the mouse oviduct, we directly exposed reproductive organs for imaging through a body wall incision (Wang and Larina, 2018a); this method of exposure is routinely used for zygotes injection during transgenic mouse production. Although this approach allowed for short-term imaging of the oviduct and gametes (Burton et al., 2015; Wang et al., 2015a; Wang and Larina, 2018b), it is not suitable for prolonged observations. Implantable optical windows are widely used in mice to bypass top tissue layers and gain imaging access to organs of interest (Alieva et al., 2014). Very recently, a similar window design was used for mid-gestation embryonic imaging with fluorescence microscopy (Huang et al., 2020). Inspired by intravital imaging of the mouse ovary (Bochner et al., 2015), we optimized a dorsal intravital window for *in vivo* prolonged and longitudinal imaging access to the mouse oviduct (Wang et al., 2018). These single-use windows are inexpensive and can be easily produced in bulk with a bench-top 3D printer. They can be autoclaved to ensure sterility.

The intravital windows are implanted through a single surgical procedure, while the imaging can be performed repeatedly under isoflurane anesthesia. As described in our previous work, the female mice with the window implanted can mate and get pregnant with embryos successfully implanted in the uterus on the window side (Moore et al., 2019), indicating that the window implantation does not have major effect on the oviductal transport of oocytes and embryos. The window with a circular aperture of 10 mm in diameter is sutured to the skin, and the ovary and oviduct are stabilized onto the tissue holders by securing the fat pad associated with the ovary with a tiny droplet of surgical glue (Figure 1A). The window is closed by a circular cover glass and secured with a C-clip or O-ring (Figure 1B). As shown in Figure 1C, the oviduct can be easily observed through the window. The window is stabilized with clamps using the frame extensions to avoid movement artifacts during

imaging. The cover glass closing the window is easily removable, which potentially allows for quick and minimally invasive access to reproductive organs for manipulations.

We implemented house-built OCT to capture oocyte/embryo dynamics through the intravital window, which is well suited for this application. The size of oocytes and embryos is ~70 μm, and the maximal luminal diameter of the oviduct ampulla with cumulus-oocyte complexes is less than 1 mm. The field of view from OCT can cover a major portion of the curled oviduct together with the ovary (Figure 1D), while the millimeter-level imaging depth covers the full oviductal lumen (Figures 1E and 1F). The micro-scale spatial resolution of OCT allows to resolve individual oocyte, embryo, cumulus cell, and detailed oviductal structures (Figures 1E and 1F). The hertz-level volumetric data acquisition rate is able to capture the cell movement with a sufficient temporal sampling. The OCT working distance of ~25 mm is convenient for positioning the animal for imaging.

We implemented this approach to image and capture unfertilized oocytes and preimplantation embryos as they are transported through the oviduct. The dynamics of unfertilized oocytes was assessed in virgin female mice, and the dynamics of preimplantation embryos was investigated in female mice after natural timed matings without exogenous hormonal stimulation. The results are grouped for specific regions within the oviduct and presented in the order of their natural transit direction, from the ovary to the uterus. The regions include the upper ampulla, the lower ampulla where oocytes/embryos are about to pass through the isthmic-ampullary junction, the isthmus, and the lower isthmus at the entry to the utero-tubal junction.

RESULTS

Fast circular movements of cumulus-oocyte complexes in the upper ampulla

Oocytes start their journey through the oviduct as a dense, viscous mass called the cumulus-oocyte complex. In OCT cross-sectional images, oocytes are distinguishable as bright white circles outlined by dark rings of zona pellucidae and surrounded by cumulus cells seen as white dots. Figure 2A shows an overall 3D OCT visualization of the oviduct with oocytes segmented out (red balls); oocytes were located close to each other and positioned in the upper ampulla. Surprisingly, time-lapse volumetric imaging revealed that cumulus-oocyte complexes in the upper ampulla were highly mobile (Figure 2B; Figure S1A; Video S1). The continuous movement of cumulus-oocyte complexes exhibited well-defined circular trajectories, completing a circle within a few minutes, and the complexes remained intact during the movement. Notably, the 3D path formed by each cumulus-oocyte complex was highly consistent over time and was spatially distinguished from the paths formed by the other complexes (Figure 2C; Video S2). Figure 2D shows an interesting example of oocyte movement pattern formed by the oocyte tracks; the oocyte movements were synchronized, and their trajectories formed circles of different diameter depending on their locations within the spinning cloud of cumulus-oocyte complexes. The average speed of oocytes ranged from 7.0 to 18.4 μm/s (Figure 2E). The quantification of the circling path perimeter demonstrates that the movements along the circles of different perimeters had different average speeds (two examples shown in Figure S2). A linear regression (Figure 2F) quantitatively confirms

that the oocyte speed is affected by the path perimeter. The longer the perimeter, the higher the speed, contributing to observed large variation of the oocyte speed.

Because the reproductive system is secured on the petals of the window, one can easily locate the same region of the oviduct over multiple imaging sessions. An example of repeated imaging in the upper ampulla over 6 h is shown in Figure 2G and Video S3, which revealed 3D dynamics of the oviductal lumen. Although the cumulus-oocyte complexes were highly dynamic, their directional progression through the upper ampulla appeared to be relatively slow. It was observed that the directional progression of oocytes was restricted by a luminal constriction throughout the downstream section of the ampulla, which formed a ‘‘gate’’ constraining the region of oocyte circling within an open section of the ampulla. The lumen of the constricted area was open to allow oviductal fluid to go through, as seen at the time point of 0 h, but the opening was too small for cumulus-oocyte complexes to pass through. Remarkably, over hours, the ‘‘gate’’ gradually opened, and the circling cloud of cumulus-oocyte complexes slowly progressed toward the lower ampulla. The panels in Figure 2G show the constricted lumen and its opening over time through different cross-sections of the volumetric data. The progression of the luminal opening was quantified by cross-sectional area measurements at two locations along the tube (Figure S3). This example clearly shows that the method can be used for quantitative imaging and assessment of oocyte movements in the context of overall luminal changes over hours, which is currently not accessible through other approaches.

Pulsatile oscillations of cumulus-oocyte complexes in the lower ampulla

After arriving in the lower ampulla, the cumulus-oocyte complexes exhibited different movement patterns. The oocytes still stayed relatively close to each other, as in the upper ampulla (Figure 3A); however, the amount of cumulus cells surrounding each oocyte was visibly reduced (Figure 3B). Time-lapse volumetric imaging revealed that the cumulus-oocyte complexes featured short-distance pulsatile oscillations with a periodicity of about 30 s (Figure 3B; Figure S1B; Video S4), while slowly progressing toward the isthmic-ampullary junction (Figures 3C and 3D). Interestingly, we observed a correlation between the isthmus luminal area change and the pulsatile oocyte movements in the lower ampulla. As shown in Figures 3E and 3F and Video S5, when the upper-isthmus luminal area increased (magenta arrows, Figure 3E), oocytes made a forward movement toward the isthmic-ampullary junction (cyan arrows, Figure 3E), and when the upper-isthmus luminal area decreased (magenta arrows, Figure 3F), oocytes moved backward in the lower ampulla (cyan arrows, Figure 3F). An overlay of the upper-isthmus luminal area (blue line) and the oocyte velocity in the lower ampulla (brown line) over time shows that these two dynamics share periodicity, with the upper-isthmus expansions consistently coinciding with the forward movements of oocytes (Figures 3G and 3H). This relationship was also confirmed by the match of frequency spectra from the two activities (Figure 3I), as well as a statistically significant slope from the linear regression of the two activities (Figure 3J). This example demonstrates the feasibility of quantitative correlative analysis of oocyte movements and luminal contractions, which are believed to be involved in the transport.

Grouping and separation of preimplantation embryos in the lower ampulla

Our imaging settings did not allow us to visualize the fertilization process or directly distinguish between unfertilized oocytes and zygotes; however, after fertilization (in mated female mice), preimplantation embryos lost cumulus cells (0.5 dpc). In Figure 4, we show the dynamics captured after fertilization, where grouping and separation of embryos are revealed in the lower ampulla. In contrast with unfertilized oocytes, preimplantation embryos were observed in cohesive groups that, despite active luminal dynamics of the oviduct, stayed relatively intact and stable at a fixed location over time (Figure 4A; Video S6). Individual embryos can separate from the group and freely move within the lower ampulla (Figure 4B; Video S7). As shown in Figure S4, the embryo separation from the group coincided with a switch of the luminal area change from negative (contraction) to positive (relaxation). Individual embryos and a group can also come together to form a larger group (Figure 4C; Video S8). As the individual embryo joined a group and continued moving together (Figure 4D), its speed markedly reduced (Figure 4E). Notably, in the lower ampulla, both the average and the maximum moving speed of the embryo group are dependent on its size (the number of embryos), as revealed by statistically significant linear-regression slopes for the speed versus the number of embryos within the group (Figure 4F). Specifically, the smaller the group, the faster the movement (Figure 4F).

Fast, long-distance forward and backward movements of preimplantation embryos in the isthmus and peristaltic waves of the isthmus luminal contraction

In the isthmus, preimplantation embryos (1.5 dpc) were relatively spread (Figure 5A) in comparison with the cohesive groups in the lower ampulla. Embryos in the isthmus exhibited fast, bi-directional movements, traveling relatively long distances over each cycle (Figure 5B; Figure S1C; Video S9). A speed map for the forward and backward movements of two embryos is shown in Figure 5C. Ultrafast volumetric imaging revealed peristaltic waves of the isthmus luminal contraction (Figure 5D; Video S10) with a wave propagation speed ranging from 0.6 to 1.2 mm/s and a contraction frequency between 0.02 and 0.06 Hz (Figure 5E).

Short-distance movements of preimplantation embryos in the lower isthmus at the entrance to the utero-tubal junction

As embryos progressed closer to the utero-tubal junction (late 1.5–2.0 dpc), their movement pattern changed significantly (Figure 6). Specifically, embryos grouped back together (Figure 6A), similar to how they were grouped in the lower ampulla. Their activities were restricted to a small region within the lower isthmus (Figure 6B). The movements featured pulsatile oscillations with small amplitudes (Video S11). The moving speed of embryos in this region, ranging from 14.7 to 60.0 μm/s (Figure 6C), was much slower in comparison with the freely moving embryos in the upper and mid-isthmus as described above.

DISCUSSION

Understanding the dynamics of oocytes/embryos and the functional roles of the oviduct *in vivo* is essential to determine the mechanisms underlying oviduct-related reproductive disorders, such as tubal ectopic pregnancy and infertility, and to achieve a further

optimization of ART. Although *ex vivo* studies provided insights into the oocyte/embryo transport in the oviduct, *in vivo* analysis has been largely absent. This imaging study revealed a number of previously unknown activities of oocytes/embryos within the oviduct *in vivo* (summarized in Figure 7), raising new hypotheses and suggesting a complex regulatory process of the oviductal transport. The presented imaging approach provides the potential to elucidate how the oviduct transports oocytes and embryos through an integration with a variety of genetic approaches, pharmacological manipulations, and mouse models.

The observed circular movements of cumulus-oocyte complexes in the upper ampulla raise multiple questions and hypotheses. As the luminal epithelium of the upper ampulla is covered by motile cilia that create micro-flows, the beat of cilia is likely a contributor of the observed circular movements of cumulus-oocyte complexes. The temporally consistent but spatially distinct oocyte trajectories in the upper ampulla reveal highly complex 3D flow fields, suggesting a possibly spatial variation of ciliary behaviors, in spite of a known coordinative nature of motile cilia (Elgeti and Gompper, 2013). It is potentially feasible to investigate the spatially resolved ciliary activities *in vivo* by a combination of the presented method with a spatial mapping of the cilia beat frequency (Wang et al., 2015a). Also, genetic or pharmacological inhibitions of the oviductal ciliary activity could be employed to determine the specific roles of cilia in producing the circular oocyte movements. Such studies will generate *in vivo* insights into the functional role of cilia in oviductal transport and uncover how large groups of cilia produce complex yet organized flow fields. To our knowledge, the circular movement of cumulus-oocyte complexes in the upper ampulla has not been previously reported *in vivo*, and its role is unclear. With the ‘‘gate’’ formed by the luminal constriction likely controlling the timing of the oocyte transport, the beat of cilia possibly generates the required force to move the cumulus-oocyte complex in the upper ampulla. This type of movement could be important for a disruption of the cumulus mass, or this might be a component of unexplored biomechanical signaling. One could also speculate that the continuous circular movement helps to prevent cells from attaching to the epithelium. Tubal pregnancies were not reported in mice; however, in humans, the beat of motile cilia might act to prevent tubal implantations by inducing continuous movements of cells, because ciliopathies are linked to a higher incidence of ectopic pregnancies (Knowles et al., 2013).

Another interesting question regarding the observed circulatory flows in the upper ampulla is related to the fact that oocytes at this location move at a speed of around 13.8 μm/s. Considering that the length of the entire mouse oviduct is about 18 mm (Agduhr, 1927), at such a high speed, the oocytes would quickly pass through the ampulla unless their forward progression is restricted by the ‘‘gate’’ of luminal constriction. Such a ‘‘gate’’ is presumably formed by a tonic oviductal smooth muscle contraction, and the opening of the ‘‘gate’’ by the slow, progressive smooth muscle relaxation, which could release oocytes toward the lower ampulla. This type of tonic contraction of smooth muscle in the mammalian oviduct was reported in some early work (Ezzati et al., 2014), which was detected by *in vitro* electrical recording (Gonzalez de Vargas et al., 1976; Talo and Brundin, 1971). Given that timing is critical for a successful fertilization, the formation of this ‘‘gate’’ may allow sufficient time for the sperm to travel through the uterus and the oviductal isthmus, thus providing an overlapping time window for the meeting of oocytes and sperm at the

fertilization site. It is reasonable to speculate that, if such a ‘‘gate’’ does not form or fails to open because of muscular disfunction, the oocytes could miss the time window of sperm arrival. Previous studies showed that blocking oviductal muscle contraction does not prevent oocyte transport to the lower ampulla (Halbert et al., 1976a, 1976b, 1989). Our *in vivo* observations agree with those findings because the observations suggest that the ampulla smooth muscle contraction functions as a ‘‘gate’’ to restrict rather than to drive the directional transfer; thus, inhibition of muscle contraction would not be expected to prevent the delivery of oocytes through the ampulla. This hypothesis could potentially be tested through combination of the presented imaging approach with targeted inhibition of smooth muscle activities.

We detected different movement patterns of oocytes in the upper and lower ampulla, suggesting different control mechanisms between these regions. It is known that the density of cilia is less in the lower ampulla compared with the upper ampulla (Wang et al., 2015a). We observed short-distance pulsatile oscillations of cumulus-oocyte complexes in the lower ampulla, which is in agreement with the previous finding of rapid to-and-fro movements of oocytes in the lower ampulla portion of the rabbit oviduct (Halbert et al., 1976b). Unexpectedly, quantitative analysis of the upper isthmus contractions and the oocyte velocity in the lower ampulla suggests their temporal correspondence. This suggests that the oscillatory movement of oocytes in the lower ampulla might be driven by upper isthmus luminal contractions. To our knowledge, such a remote pumping mechanism driving oviductal transport has not been previously proposed. This observation does not exclude the possibility that the ciliary beat in the lower ampulla contributes to the slow progression of oocytes toward the isthmic-ampullary junction, and the oscillations by themselves do not produce net forward movement. This process could be further explored by genetic or pharmacological manipulation of cilia and smooth muscle dynamics in the oviduct and the presented imaging method.

Preimplantation embryos in the lower ampulla have been detected in groups, which remain stable despite the oviduct contractions. For embryo separation from the group, assessment of the embryo dynamics in relation to the luminal area change suggests that the oviductal contraction and relaxation could be a factor affecting the embryo movement and the group separation activity. Previous *in vitro* studies demonstrated that the grouping of preimplantation embryos has a positive effect on their development, particularly in transitioning to the blastocysts stage (Buemo et al., 2016; Lee et al., 2007), and the mechanism of forming such groups was investigated (Lehtonen et al., 1984). Although embryo grouping might not be relevant to humans, this study reveals *in vivo* observation of this phenomenon in mice, setting a platform for investigation of embryo grouping in the native environment.

Unlike the lower ampulla where preimplantation embryos are in cohesive groups, in the upper and mid-isthmus, embryos appear to be separated and moving individually. From the lower ampulla to the isthmus, embryos need to pass through the isthmic-ampullary junction that has a relatively small luminal opening. The cross-sectional luminal area at the isthmic-ampullary junction under the relaxed condition (most expanded state) is ~0.018 mm^2 (mean value from three mice). By counting only the central region above the tips of mucosa folds

and approximating this region as circular, the diameter of the luminal opening can be estimated as ~92 μm (mean value from three mice), which is not large enough to allow for more than one embryo to simultaneously pass through. Specifically, we observed that groups of embryos did not directly pass through the isthmic-ampullary junction as a whole (Videos S12 and S13; Figures S5 and S6), although they were continuously driven to the junction by oviductal activities. During this dynamic, an individual embryo separated from the group was observed being transported within the isthmic-ampullary junction, featuring both forward and backward movements (Video S13; Figure S6). Observations of unfertilized oocytes surrounded by cumulus cells show repeated forward and backward movements inside the narrow lumen of the isthmic-ampullary junction, which is similar to the transport of embryos observed at this region. These suggest that there likely exists another ‘‘gate’’ at the isthmic-ampullary junction limiting the size of the passage to the individual oocytes/embryos. The ‘‘gate,’’ as well as oviductal contractions driving oocytes and embryos through the junction, could contribute to separation of groups. Enabled by the *in vivo* imaging approach, these observations of the mammalian oocyte/embryo transport at the isthmic-ampullary junction set the stage to study the underlying mechanisms, which could potentially contribute to understanding the causes of embryo retention in the oviduct. Future investigations with targeted control of the oviductal muscular activity at the anatomical boundaries could elucidate the functional role of the oviduct in transporting oocytes and embryos through the boundary regions under normal and disordered conditions.

We detected fast, long-distance forward and backward movements of embryos in the isthmus under peristaltic luminal contraction waves. Because this region of the oviduct has little to no motile cilia (Wang et al., 2015a), this is likely a result of the myoelectric activity of smooth muscle cells, which propagate in both directions (Ezzati et al., 2014). The bi-directional movement of cells in the isthmus was previously reported with bright-field and epi-fluorescence microscopy (Bochner et al., 2015; Ishikawa et al., 2016), although not volumetrically. Implementation of 3D *in vivo* imaging of embryos in the isthmus enables measurements of the cell velocity volumetrically through direct tracking. Although preimplantation embryos appear relatively spread out as they move through the upper and mid-isthmus, they group back together and dramatically reduce the amplitude of movements as they reach the lower isthmus. This is likely because the utero-tubal junction is gated by a luminal constriction, restricting the embryos within a small region, which might improve the timing of embryo transport to the uterus once the junction opens. How embryos are transported through the utero-tubal junction and how the timing of this process is regulated can potentially be investigated using the presented method.

Our imaging observations suggest that the preimplantation embryos in the lower ampulla and the isthmus experience significant mechanical stress from shear force and movement, which could be instructive for further optimizing ART success. Current ART optimization has mainly focused on the chemical components of oviductal secretions (Avilés et al., 2010; Chronopoulou and Harper, 2015), while the role of physical factors received much less attention (Smith et al., 2012). It was shown that vibrations could be beneficial for enhancement of embryonic development and can improve implantation rate (Isachenko et al., 2010, 2011; Mizobe et al., 2010), suggesting that implementation of mechanical stimulations into ART is also a promising approach. Detailed quantitative assessment of

mechanical stresses that embryos are exposed to throughout preimplantation stages will allow for replication of the natural biomechanical settings *in vitro*. Although there are a number of objective differences between reproductive processes in mice and humans, including the number of embryos, this approach could still be potentially beneficial for ART success.

The presented imaging study was performed in female mice anesthetized through isoflurane inhalation, which might potentially have an influence on observed oviductal dynamics. This anesthesia method is widely used for *in vivo* mouse imaging (Alieva et al., 2014; Bochner et al., 2015; Huang et al., 2020), including the recent functional live studies on the oviductal fluid flow and sperm dynamics (Hino and Yanagimachi, 2019; Muro et al., 2016). The effect of isoflurane inhalation on the mouse oviductal function is currently unclear. In fact, because the anesthesia is required for *in vivo* high-resolution imaging of the mouse oviduct, a study to determine such an effect could be very challenging, where the proper control with no anesthesia is unavailable. To partially address this issue, we performed an *in vivo* assessment of the mouse oviductal cilia activity by measuring the ciliary beat frequency at the same locations of the oviduct *in vivo* at different levels of isoflurane delivered by inhalation (maintained in steps at the levels from 1% to 5% and back), which revealed constant ciliary beat frequency regardless of the level of isoflurane. Nevertheless, when interpreting the *in vivo* imaging data, the unknown potential effect from the isoflurane anesthesia should not be disregarded.

This study used one of the common mouse strains, CD-1, to demonstrate the *in vivo* imaging approach and present the previously unknown cell activities in the oviduct. For both wild-type and mutant mice, genetic background could influence reproductive phenotypes (Silver, 1995; Wang et al., 2004b). Thus, strain-related differences in the dynamics of oocytes/embryos within the oviduct are possible, which might be because of potential differences in any physiological characteristics regulating the female reproductive system, such as hormonal levels. Future assessments of strain-related variations in the oviductal transport process using the described *in vivo* imaging approach could potentially address this question.

Imaging capabilities is a major limiting factor determining what can be studied in mammalian reproduction (Burton et al., 2015; Daloglu and Ozcan, 2017; Kölle et al., 2009; Trottmann et al., 2016). The presented approach for *in vivo* volumetric imaging of oocyte/embryo dynamics inside the oviduct opens an avenue to answer critical questions that were previously impossible or very difficult to approach, for example, determining the dynamic role of oviduct in the oocyte/embryo transport and the mechanism underlying tubal embryo retentions. Ovulation and oocyte transport to the ampulla is another important aspect of the reproductive process to investigate. Also, the communications or interactions between gametes/embryos and the oviduct is an emerging research area that attracts increasing interest and attention (Almiñana, 2015; Avilés et al., 2015; Coy et al., 2012; Lee and Yeung, 2006). In particular, the presence of sperm or semen in the oviduct was shown to be a modulator influencing the oviductal environment, including molecular and biochemical changes (Georgiou et al., 2007; Steinberger et al., 2017). These could potentially influence the described dynamic behaviors and the overall transport process of the oviduct.

Determining this possible effect is a focus of our future studies using the *in vivo* imaging approach, which will provide a further understanding on the role of gamete-oviduct interaction in regulating the oviductal function. Complementing the existing molecular-level investigations (Buhi et al., 1997; Coy et al., 2008; Georgiou et al., 2005; Ghersevich et al., 2015) and combined with genetic or pharmacological manipulations (Ishikawa et al., 2016; Wang et al., 2004a), the presented imaging approach creates opportunities to understand the interplay between molecular and mechanical factors in oviductal physiology and early embryonic development (Ferraz et al., 2017; Suarez, 2016). Moreover, in combination with the previously reported *in vivo* OCT-based sperm tracking and ciliary beat mapping techniques (Wang et al., 2015a; Wang and Larina, 2018b), a powerful imaging tool set is now available for a complete *in vivo* assessment of the mouse oviduct. In addition, this imaging platform can be utilized as an *in vivo* screening assay to assess the effects of clinically relevant treatments (such as hormonal stimulations) and newly developed contraceptives on the oviductal behaviors and its transporting function, providing insights into the potential influence on fertility and pregnancy.

The OCT technology is under a rapid development, and future technical advances can greatly benefit the reproductive biology research. The imaging depth of our current OCT system covers the entire lumen of the oviduct, and the spatial resolution clearly distinguishes individual oocytes, embryos, and cumulus cells. However, it requires a careful orientation of the sample and does not capture the whole length of the oviduct because of its complex spatial organization. An extended imaging depth can be achieved by implementation of a light source centered at a longer wavelength, such as at ~1,000 or ~1,300 nm, which reduces optical absorption from blood and optical scattering from tissue (Ishida and Nishizawa, 2012). Further improvement of the spatial resolution is possible by broadening the wavelength range of the light source and employing a higher magnification objective for microscopic imaging (Aguirre et al., 2015; Liu et al., 2011). Recently, with OCT, visualizing the intracellular structure of oocytes and preimplantation embryos has been demonstrated (Karnowski et al., 2017; Moore et al., 2019), leading to the capability of staging preimplantation development *in vivo* inside the mouse oviduct (Moore et al., 2019). Thus, it may be possible to identify the developmental stage of preimplantation embryos simultaneously with the dynamic imaging of their transport. The A-scan rate of the OCT system in this study was the major limitation to achieve a faster acquisition and a larger field of view. Through recent advancements in OCT technology, the A-line imaging speed can reach MHz level (Wang et al., 2015b) in comparison with the ~68 kHz in this study. This ultrahigh imaging speed could potentially reveal more temporal characteristics of the oocyte/embryo dynamics, for example, further details of cell oscillations in the lower ampulla, isthmic-ampullary junction, and isthmus. Implementation of all these advancements brings the potential to image the entire mouse oviduct, both the ampulla and the isthmus, with a high volumetric acquisition rate, while maintaining high pixel density and resolution. Such an improvement could further elucidate the coordinative activities between the ampulla and the isthmus in a successful oocyte/embryo transport, which could not be addressed in this study.

To summarize, we present *in vivo* dynamic volumetric imaging of the oviductal transport in the mouse model at a micro-scale spatial resolution. The imaging data revealed previously

unknown movements of oocytes and preimplantation embryos in their native oviductal environment. These observations suggest a complex, spatially dependent regulatory process controlling the oviductal transport of oocytes and embryos. The presented *in vivo* imaging approach creates a platform for a variety of studies investigating underlying mechanisms in normal and pathological oviductal functions, as well as preimplantation development, contributing to a better management of infertilities and other reproductive disorders.

STAR★METHODS

RESOURCE AVAILABILITY

Lead contact—Further information and requests for resources and reagents should be directed to and will be fulfilled by the Lead Contact, Irina V. Larina (larina@bcm.edu).

Materials availability—This study did not generate new unique reagents.

Data and code availability—All data in this study are available upon request.

EXPERIMENTAL MODEL AND SUBJECT DETAILS

Experimental Animals—All animal procedures have been approved by the Institutional Animal Care and Use Committee at Baylor College of Medicine, and all experiments followed the approved guidelines and regulations. Experiments were performed on wild-type CD-1 female mice (age > 6 weeks, Strain Code 022, Charles River).

METHOD DETAILS

Surgical implantation of dorsal intravital window—The imaging window was implanted on the right dorsal side of the female mouse through sterile surgery. The windows were produced on a high-resolution 3D printer with gray resin (Formlabs). These windows are disposable and autoclavable. The window design featured a clear aperture of 10 mm in diameter for the optical imaging access; detailed information on the window dimension can be found in our previous work (Wang et al., 2018). The mouse was anesthetized by isoflurane inhalation and placed on a 37°C platform. The site for window implantation was processed for hair removal and skin disinfection. A circular part of skin tissue with ~1 cm diameter was removed, and the window was sutured to the edge of the skin through 14 eyelets along the rim using 4–0 Nylon suture. Once the window frame was implanted, the muscle layer underneath the window aperture was cut for a ~2 mm incision to expose the reproductive organs. The ovary, the oviduct, and part of the uterus were gently pulled out of the body cavity and were stabilized by securing the fat pad associated with the ovary onto the window tissue holders using a tiny droplet of surgical glue. The window aperture was closed by a 12-mm-diameter circular cover glass and secured with a C-clip or O-ring. A thin, light metal cover was used to protect the window from potential chewing by the female mouse. Further details of the surgical procedure can be found in our previous work (Moore et al., 2019; Wang et al., 2018).

***In vivo* imaging with OCT—**Imaging was performed with the mouse under isoflurane anesthesia placed on a heating platform to maintain the body temperature at 37°C. A house-

built spectral domain OCT system was used in this study. Details of the system can be found in our previous work (Burton et al., 2015). Briefly, the system employs a broadband laser centered at ~810 nm with a spectral bandwidth of ~100 um. It utilizes a fiber-based Michelson interferometer for low-coherence interferometry, providing an axial resolution of ~5 μm in tissue, a transverse resolution of ~4 μm, and an imaging depth covering the entire oviductal lumen. OCT imaging was conducted through the circular cover glass on the dorsal window that was stabilized by clamping the frame extensions. For all experiments, the A-scan (in-depth line) rate of the OCT system was set at ~68 kHz. Different combinations of the volume dimensions (the number of A-lines per B-scan image and the number of B-scans per volume) were used to achieve a desired volume rate, which was up to 4 Hz. Different types of data acquisition were performed, including a single 3D imaging that covers a large transverse field of view, a time-lapse continuous 3D acquisition for a 4D imaging, and a repeated 4D acquisition over certain time intervals for a 5D imaging.

Image volumetric rendering and visualization—The Imaris software (Oxford Instruments) was utilized for reconstruction and rendering of 3D, 4D, and 5D datasets. Clipping plane function was used to present the cross-sectional views through the volume. The spot function was used to highlight oocytes/embryos in red color inside the oviductal lumen, and the spot tracking function was utilized to produce trajectories of oocytes and embryos.

QUANTIFICATION AND STATISTICAL ANALYSIS

Quantification of oocyte/embryo movement and oviductal dynamics—From the 4D datasets, the measurements of oocyte/embryo velocity and speed were obtained based on cell tracking performed in Imaris. The time-resolved speed profile, average speed, and maximum speed were directly obtained. The direction of cell movement with respect to the lumen was identified through analyzing the x, y, and z velocity vectors provided by the software. For measuring the perimeter of the oocyte circling path in the upper ampulla, 3D positions of the oocyte over one circle were exported from Imaris, which were smoothed in 3D, as shown in Figure S2. The length of the smoothed 3D trajectory was then measured as the perimeter of the oocyte circling path. For quantification of the oviductal dynamics, the luminal area was measured by segmentation in ImageJ. The contraction and relaxation of the oviduct lumen were examined by the luminal area change as the first derivative of the luminal area over time. The luminal contraction wave speed was determined by a spatiotemporal assessment of the luminal area change along the tube as detailed in our previous work (Wang et al., 2018).

Statistical Analysis—All statistical details are indicated in the figure panels and figure legends. The statistics of linear regression was performed in OriginPro (OriginLab) with an α value of 0.05.

Supplementary Material

Refer to Web version on PubMed Central for supplementary material.

ACKNOWLEDGMENTS

We would like to thank Profs. Richard R. Behringer (University of Texas MD Anderson Cancer Center), Ross A. Poché (Baylor College of Medicine), and Wipawee Winuthayanon (Washington State University) for their critical reading of the manuscript. This study was supported by NIH grants (R21EB028409 to S.W.; R01HL120140, R01EB027099, and R01HD096335 to I.V.L.), as well as the Start-Up Funds from Stevens Institute of Technology (to S.W.). We thank the Optical Imaging & Vital Microscopy Core at Baylor College of Medicine for technical support.

REFERENCES

Agduhr E (1927). Studies on the Structure and Development of the Bursa Ovarica and the Tuba Uterina in the Mouse. Acta Zoologica 8, 1–133.

Aguirre AD, Zhou C, Lee H-C, Ahsen OO, and Fujimoto JG (2015). Optical coherence microscopy. In Optical Coherence Tomography: Technology and Applications, Drexler W and Fujimoto JG, eds. (Springer International Publishing), pp. 865–911.

Alieva M, Ritsma L, Giedt RJ, Weissleder R, and van Rheenen J (2014). Imaging windows for long-term intravital imaging: General overview and technical insights. Intravital 3, e29917. [PubMed: 28243510]

Almiñana C (2015). Snooping on a private conversation between the oviduct and gametes/embryos. Anim. Reprod 12, 366–374.

Avilés M, Gutiérrez-Adán A, and Coy P (2010). Oviductal secretions: will they be key factors for the future ARTs? Mol. Hum. Reprod 16, 896–906. [PubMed: 20584881]

Avilés M, Coy P, and Rizos D (2015). The oviduct: A key organ for the success of early reproductive events. Anim. Front 5, 25–31.

Battalia DE, and Yanagimachi R (1979). Enhanced and co-ordinated movement of the hamster oviduct during the periovulatory period. J. Reprod. Fertil 56, 515–520. [PubMed: 573324]

Besenfelder U, Havlicek V, and Brem G (2012). Role of the oviduct in early embryo development. Reprod. Domest. Anim 47 (Suppl 4), 156–163.

Bochner F, Fellus-Alyagor L, Kalchenko V, Shinar S, and Neeman M (2015). A Novel Intravital Imaging Window for Longitudinal Microscopy of the Mouse Ovary. Sci. Rep 5, 12446. [PubMed: 26207832]

Buemo CP, Gambini A, Moro LN, Hiriart MI, Fernández-Martín R, Collas P, and Salamone DF (2016). Embryo Aggregation in Pig Improves Cloning Efficiency and Embryo Quality. PLoS ONE 11, e0146390. [PubMed: 26894831]

Buhi WC, Alvarez IM, and Kouba AJ (1997). Oviductal regulation of fertilization and early embryonic development. J. Reprod. Fertil. Suppl 52, 285–300. [PubMed: 9602736]

Burton JC, Wang S, Stewart CA, Behringer RR, and Larina IV (2015). High-resolution three-dimensional in vivo imaging of mouse oviduct using optical coherence tomography. Biomed. Opt. Express 6, 2713–2723. [PubMed: 26203393]

Chronopoulou E, and Harper JC (2015). IVF culture media: past, present and future. Hum. Reprod. Update 21, 39–55. [PubMed: 25035437]

Coy P, Cánovas S, Mondéjar I, Saavedra MD, Romar R, Grullón L, Matás C, and Avilés M (2008). Oviduct-specific glycoprotein and heparin modulate sperm-zona pellucida interaction during fertilization and contribute to the control of polyspermy. Proc. Natl. Acad. Sci. USA 105, 15809–15814. [PubMed: 18838686]

Coy P, García-Vázquez FA, Visconti PE, and Avilés M (2012). Roles of the oviduct in mammalian fertilization. Reproduction 144, 649–660. [PubMed: 23028122]

Daloglu MU, and Ozcan A (2017). Computational imaging of sperm locomotion. Biol. Reprod 97, 182–188. [PubMed: 29044431]

Elgeti J, and Gompper G (2013). Emergence of metachronal waves in cilia arrays. Proc. Natl. Acad. Sci. USA 110, 4470–4475. [PubMed: 23487771]

Ezzati M, Djahanbakhch O, Arian S, and Carr BR (2014). Tubal transport of gametes and embryos: a review of physiology and pathophysiology. J. Assist. Reprod. Genet 31, 1337–1347. [PubMed: 25117646]

Fauci LJ, and Dillon R (2006). Biofluidmechanics of reproduction. Annu. Rev. Fluid Mech 38, 371–394.

Ferraz MAMM, Henning HHW, Stout TAE, Vos PLAM, and Gadella BM (2017). Designing 3-Dimensional In Vitro Oviduct Culture Systems to Study Mammalian Fertilization and Embryo Production. Ann. Biomed. Eng 45, 1731–1744. [PubMed: 27844174]

Georgiou AS, Sostaric E, Wong CH, Snijders APL, Wright PC, Moore HD, and Fazeli A (2005). Gametes alter the oviductal secretory proteome. Mol. Cell. Proteomics 4, 1785–1796. [PubMed: 16105986]

Georgiou AS, Snijders APL, Sostaric E, Aflatoonian R, Vazquez JL, Vazquez JM, Roca J, Martinez EA, Wright PC, and Fazeli A (2007). Modulation of the oviductal environment by gametes. J. Proteome Res 6, 4656–4666. [PubMed: 18004800]

Ghersevich S, Massa E, and Zumoffen C (2015). Oviductal secretion and gamete interaction. Reproduction 149, R1–R14. [PubMed: 25190504]

Gonzalez de Vargas MI, Talo A, and Hodgson BJ (1976). Correlation between intraluminal pressure of the oviduct and the electrical activity of the longitudinal peritoneal muscle in the rabbit. Biol. Reprod 15, 492–496. [PubMed: 974202]

Halbert SA, Tam PY, and Blandau RJ (1976a). Egg transport in the rabbit oviduct: the roles of cilia and muscle. Science 191, 1052–1053. [PubMed: 1251215]

Halbert SA, Tam PY, Adams RJ, and Blandau RJ (1976b). An analysis of the mechanisms of egg transport in the ampulla of the rabbit oviduct. Gynecol. Invest 7, 306–320. [PubMed: 1001998]

Halbert SA, Becker DR, and Szal SE (1989). Ovum transport in the rat oviductal ampulla in the absence of muscle contractility. Biol. Reprod 40, 1131–1136. [PubMed: 2775809]

Hino T, and Yanagimachi R (2019). Active peristaltic movements and fluid production of the mouse oviduct: their roles in fluid and sperm transport and fertilizationy. Biol. Reprod 101, 40–49. [PubMed: 30977810]

Horne AW, Phillips JA 3rd, Kane N, Lourenco PC, McDonald SE, Williams AR, Simon C, Dey SK, and Critchley HO (2008). CB1 expression is attenuated in Fallopian tube and decidua of women with ectopic pregnancy. PLoS ONE 3, e3969. [PubMed: 19093002]

Huang D, Swanson EA, Lin CP, Schuman JS, Stinson WG, Chang W, Hee MR, Flotte T, Gregory K, Puliafito CA, et al. (1991). Optical coherence tomography. Science 254, 1178–1181. [PubMed: 1957169]

Huang Q, Cohen MA, Alsina FC, Devlin G, Garrett A, McKey J, Havlik P, Rakhilin N, Wang E, Xiang K, et al. (2020). Intravital imaging of mouse embryos. Science 368, 181–186. [PubMed: 32273467]

Isachenko E, Maettner R, Isachenko V, Roth S, Kreienberg R, and Sterzik K (2010). Mechanical agitation during the in vitro culture of human pre-implantation embryos drastically increases the pregnancy rate. Clin. Lab 56, 569–576. [PubMed: 21141442]

Isachenko V, Maettner R, Sterzik K, Strehler E, Kreinberg R, Hancke K, Roth S, and Isachenko E (2011). In-vitro culture of human embryos with mechanical micro-vibration increases implantation rates. Reprod. Biomed Online 22, 536–544.

Ishida S, and Nishizawa N (2012). Quantitative comparison of contrast and imaging depth of ultrahigh-resolution optical coherence tomography images in 800–1700 nm wavelength region. Biomed. Opt. Express 3, 282–294. [PubMed: 22312581]

Ishikawa Y, Usui T, Yamashita M, Kanemori Y, and Baba T (2016). Surfing and Swimming of Ejaculated Sperm in the Mouse Oviduct. Biol. Reprod 94, 89. [PubMed: 26962118]

Karnowski K, Ajduk A, Wieloch B, Tamborski S, Krawiec K, Wojtkowski M, and Szkulmowski M (2017). Optical coherence microscopy as a novel, non-invasive method for the 4D live imaging of early mammalian embryos. Sci. Rep 7, 4165. [PubMed: 28646146]

Knowles MR, Daniels LA, Davis SD, Zariwala MA, and Leigh MW (2013). Primary ciliary dyskinesia. Recent advances in diagnostics, genetics, and characterization of clinical disease. Am. J. Respir. Crit. Care Med 188, 913–922. [PubMed: 23796196]

Kölle S, Dubielzig S, Reese S, Wehrend A, König P, and Kummer W (2009). Ciliary transport, gamete interaction, and effects of the early embryo in the oviduct: ex vivo analyses using a new digital videomicroscopic system in the cow. Biol. Reprod 81, 267–274. [PubMed: 19299315]

Lee KF, and Yeung WS (2006). Gamete/embryo - oviduct interactions: implications on in vitro culture. Hum. Fertil. (Camb.) 9, 137–143. [PubMed: 17008265]

Lee SG, Park CH, Choi DH, Kim HS, Ka HH, and Lee CK (2007). In vitro development and cell allocation of porcine blastocysts derived by aggregation of in vitro fertilized embryos. Mol. Reprod. Dev 74, 1436–1445. [PubMed: 17440970]

Lehtonen E, Wartiovaara J, and Reima I (1984). Cell relationships during aggregation between preimplantation embryos and teratocarcinoma-derived cells. J. Embryol. Exp. Morphol 81, 17–35. [PubMed: 6470607]

Li S, and Winuthayanon W (2017). Oviduct: roles in fertilization and early embryo development. J. Endocrinol 232, R1–R26. [PubMed: 27875265]

Liu L, Gardecki JA, Nadkarni SK, Toussaint JD, Yagi Y, Bouma BE, and Tearney GJ (2011). Imaging the subcellular structure of human coronary atherosclerosis using micro-optical coherence tomography. Nat. Med 17, 1010–1014. [PubMed: 21743452]

Lyons RA, Saridogan E, and Djahanbakhch O (2006). The reproductive significance of human Fallopian tube cilia. Hum. Reprod Update 12, 363–372.

Menezo Y, and Guerin P (1997). The mammalian oviduct: biochemistry and physiology. Eur. J. Obstet. Gynecol. Reprod. Biol 73, 99–104. [PubMed: 9175697]

Ménézo Y, Guérin P, and Elder K (2015). The oviduct: a neglected organ due for re-assessment in IVF. Reprod. Biomed Online 30, 233–240.

Mizobe Y, Yoshida M, and Miyoshi K (2010). Enhancement of cytoplasmic maturation of in vitro-matured pig oocytes by mechanical vibration. J. Reprod. Dev 56, 285–290. [PubMed: 20103989]

Moore EL, Wang S, and Larina IV (2019). Staging mouse preimplantation development in vivo using optical coherence microscopy. J. Biophotonics 12, e201800364. [PubMed: 30578614]

Muro Y, Hasuwa H, Isotani A, Miyata H, Yamagata K, Ikawa M, Yanagimachi R, and Okabe M (2016). Behavior of Mouse Spermatozoa in the Female Reproductive Tract from Soon after Mating to the Beginning of Fertilization. Biol. Reprod 94, 80. [PubMed: 26962112]

Shaw JLV, Dey SK, Critchley HOD, and Horne AW (2010). Current knowledge of the aetiology of human tubal ectopic pregnancy. Hum. Reprod Update 16, 432–444.

Silver LM (1995). Mouse Genetics: Concepts and Applications (Oxford University Press).

Smith GD, Takayama S, and Swain JE (2012). Rethinking In Vitro Embryo Culture: New Developments in Culture Platforms and Potential to Improve Assisted Reproductive Technologies. Biol. Reprod 86, 62. [PubMed: 21998170]

Spassky N, and Meunier A (2017). The development and functions of multiciliated epithelia. Nat. Rev. Mol. Cell Biol 18, 423–436. [PubMed: 28400610]

Steinberger B, Yu H, Brodmann T, Milovanovic D, Reichart U, Besenfelder U, Artemenko K, Razzazi-Fazeli E, Brem G, and Mayrhofer C (2017). Semen modulated secretory activity of oviductal epithelial cells is linked to cellular proteostasis network remodeling: Proteomic insights into the early phase of interaction in the oviduct in vivo. J. Proteomics 163, 14–27. [PubMed: 28495501]

Suarez SS (2016). Mammalian sperm interactions with the female reproductive tract. Cell Tissue Res 363, 185–194. [PubMed: 26183721]

Talo A, and Brundin J (1971). Muscular activity in the rabbit oviduct: a combination of electric and mechanic recordings. Biol. Reprod 5, 67–77. [PubMed: 5128203]

Trottmann M, Sroka R, Stepp H, Liedl B, Becker AJ, Stief CG, and Kölle S (2016). Probe-based confocal laser endomicroscopy (pCLE): a pre-clinical investigation of the male genital tract. Lasers Med. Sci 31, 57–65. [PubMed: 26519156]

Wang S, and Larina IV (2018a). In vivo imaging of the mouse reproductive organs, embryo transfer, and oviduct cilia dynamics using optical coherence tomography. In Mouse Embryogenesis: Methods and Protocols, Olguin PD, ed. (Humana Press, Springer Nature).

Wang S, and Larina IV (2018b). In vivo three-dimensional tracking of sperm behaviors in the mouse oviduct. Development 145, dev157685. [PubMed: 29487107]

Wang H, Guo Y, Wang D, Kingsley PJ, Marnett LJ, Das SK, DuBois RN, and Dey SK (2004a). Aberrant cannabinoid signaling impairs oviductal transport of embryos. Nat. Med 10, 1074–1080. [PubMed: 15378054]

Wang H, Ma WG, Tejada L, Zhang H, Morrow JD, Das SK, and Dey SK (2004b). Rescue of female infertility from the loss of cyclooxygenase-2 by compensatory up-regulation of cyclooxygenase-1 is a function of genetic makeup. J. Biol. Chem 279, 10649–10658. [PubMed: 14701858]

Wang S, Burton JC, Behringer RR, and Larina IV (2015a). In vivo micro-scale tomography of ciliary behavior in the mammalian oviduct. Sci. Rep 5, 13216. [PubMed: 26279472]

Wang S, Singh M, Lopez AL 3rd, Wu C, Raghunathan R, Schill A, Li J, Larin KV, and Larina IV (2015b). Direct four-dimensional structural and functional imaging of cardiovascular dynamics in mouse embryos with 1.5 MHz optical coherence tomography. Opt. Lett 40, 4791–4794. [PubMed: 26469621]

Wang S, Syed R, Grishina OA, and Larina IV (2018). Prolonged in vivo functional assessment of the mouse oviduct using optical coherence tomography through a dorsal imaging window. J. Biophotonics 11, e201700316. [PubMed: 29359853]

Highlights

- Dynamic 3D imaging of oocyte/embryo transport in the mouse oviduct *in vivo*
- Quantitative assessment of oocyte/embryo movement and oviductal activities
- Circling movement of cumulus-oocyte complexes in the upper ampulla
- Grouping and separation of preimplantation embryos in the lower ampulla

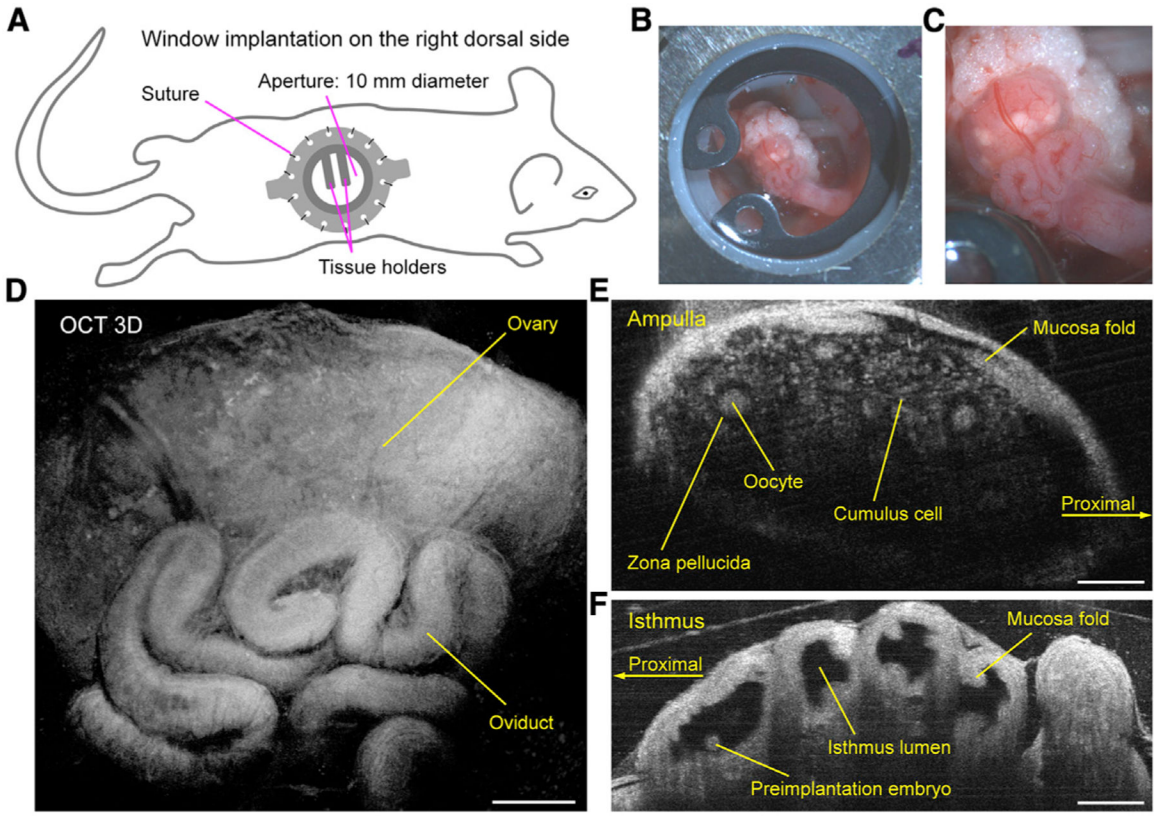

Figure 1. High-resolution 3D imaging of the mouse oviduct with OCT through a dorsal intravital window

(A) Illustration for dorsal implantation of the window.

(B) Image of the window setup and the reproductive organs *in vivo*.

(C) Bright-field visualization of the oviduct through the dorsal window *in vivo*.

(D) 3D OCT imaging of the mouse oviduct and ovary through the dorsal window *in vivo*.

(E) Cross-section of *in vivo* 3D OCT image at the ampulla shows oocytes surrounded by cumulus cells.

(F) Cross-section of *in vivo* 3D OCT image at the isthmus shows the preimplantation embryo. Scale bars: 200 μm (D and E); 300 μm (F).

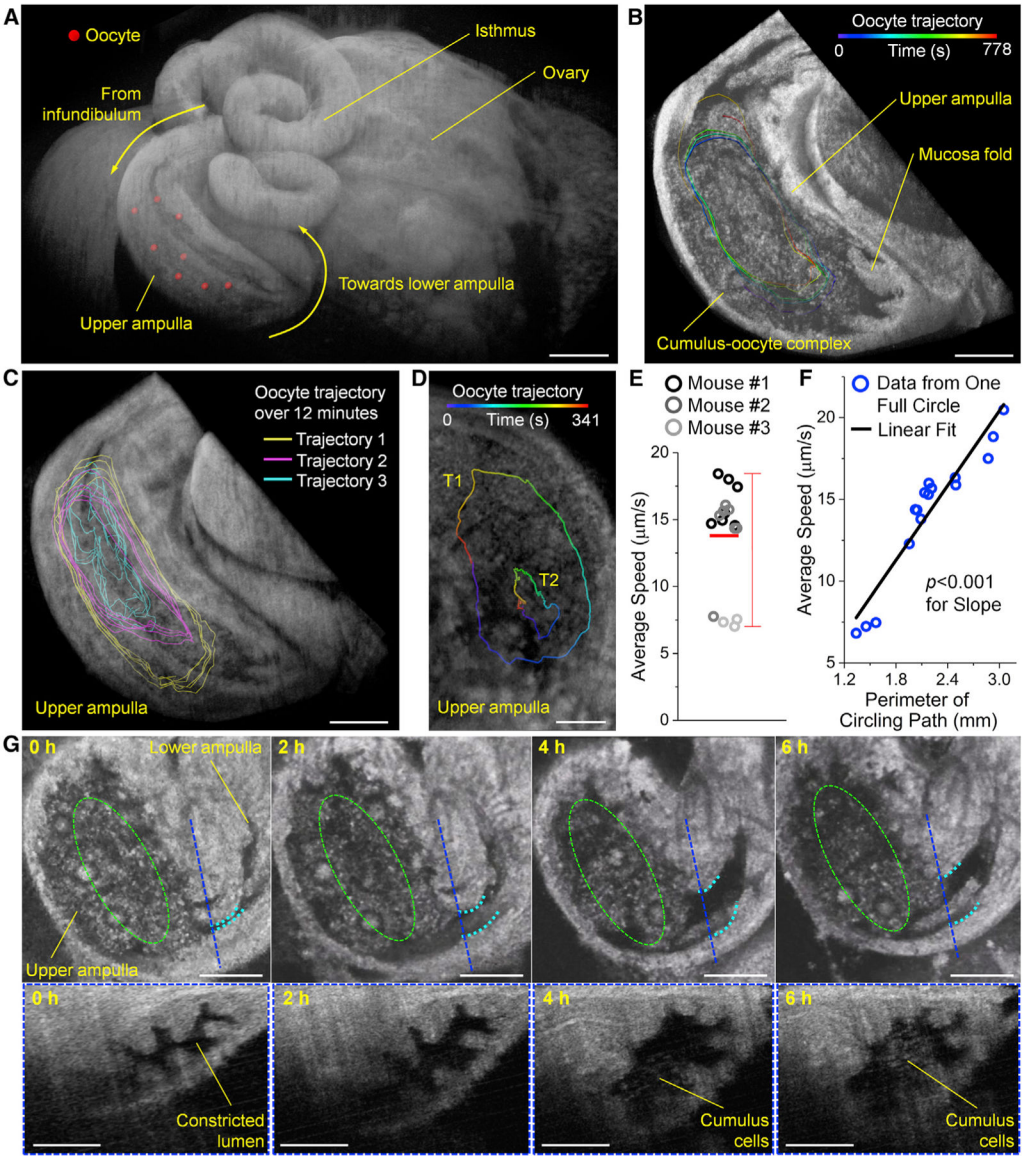

Figure 2. Circular movement of cumulus-oocyte complexes in the upper ampulla

(A) Volumetric view shows the location of oocytes in the upper ampulla.

(B and C) Corresponding cross-sectional 3D image shows (B) cumulus-oocyte complexes and a trajectory of oocyte movement (Video S1), as well as (C) relative positions of three representative oocyte trajectories in the upper ampulla (Video S2).

(D) Two oocyte trajectories in the upper ampulla show synchronized outer and inner circular movements.

(E) Average speed of oocyte movements in the upper ampulla. Red line: mean; whiskers: range.

(F) Linear regression of the average speed versus the perimeter of oocyte circling movement in the upper ampulla shows a statistically significant dependence.

(G) Cross-sections through volumetric time lapses at 2-h intervals show constriction of the oviductal lumen, forming a ‘‘gate’’ (cyan double dashed lines) and restricting the region of

circling cumulus-oocyte complexes (green dashed circles), as well as the gradual opening of the ‘‘gate’’ over the period of 6h (Video S3). Blue dashed lines in the top panels indicate the locations of cross-sections in the bottom panel. Scale bars: 500 μm (A); 300 μm (B, C, and G, top panels); 200 μm (D and G, bottom panels).

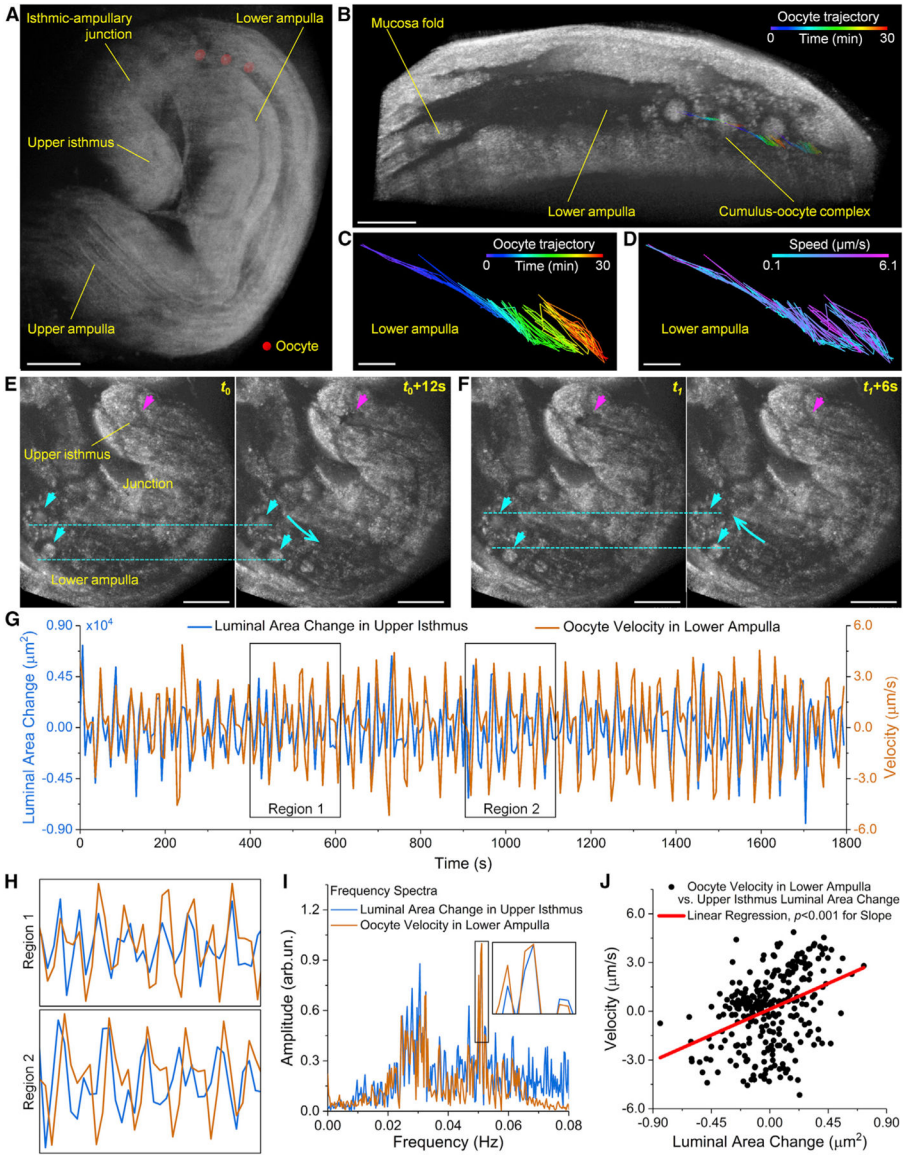

Figure 3. Pulsatile oscillations and slow forward progression of oocytes in the lower ampulla

(A) Volumetric OCT view shows the location of oocytes in the lumen of the lower ampulla, close to the isthmic-ampullary junction.

(B) Cross-section of the 3D volumetric time lapse with labeled oocyte trajectories. The trajectories are color coded according to time. The oocytes with the remaining cumulus cells exhibited pulsatile oscillations with a slow forward progression over time (Video S4). Such pulsatile oscillations of oocytes were observed in two mice.

(C and D) Zoom-in views of a representative oocyte trajectory color-coded for (C) time and (D) oocyte speed.

(E and F) Cross-sectional 3D views along the lumen of the lower ampulla and also covering the upper isthmus. Directions of the oocyte movement are labeled with long cyan arrows. (E) Opening of the lumen in the upper isthmus (short magenta arrow) corresponded to a forward movement of oocytes (short cyan arrows) toward the isthmic-ampullary junction, while (F)

closing of the lumen in the upper isthmus showed correspondence to a backward movement of oocytes in the lower ampulla. Dynamics of such movements can be visualized in Video S5.

(G) Overlay of the upper-isthmus luminal area change (blue line) and the oocyte velocity in the lower ampulla (brown line) over time shows that the isthmus expansions consistently corresponded to the forward movements of oocytes.

(H) Zoom-in views of the plot from two regions labeled in (G).

(I) Overlaid plots of frequency spectra of luminal area change and oocyte velocity (obtained by fast Fourier transform) show a good overlap between the peaks.

(J) Linear regression of the oocyte velocity in the lower ampulla versus the luminal area change in the upper isthmus shows the correlation of the two activities. Scale bars: 300 μm (A); 200 μm (B); 30 μm (C and D); 250 μm (E and F).

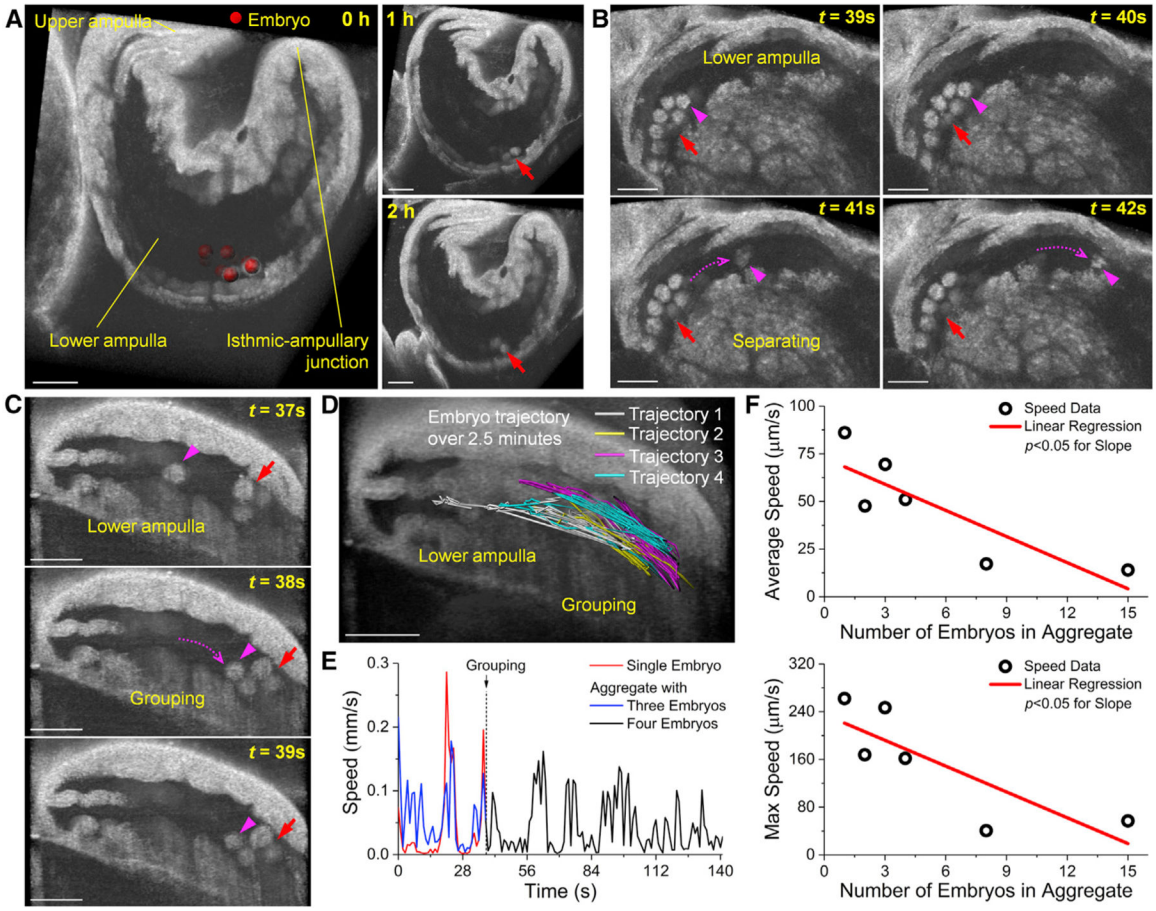

Figure 4. Embryo grouping, separation, and movement of the embryo group in the lower ampulla

(A) Cross-sectional 3D image shows the widely open lower-ampulla lumen with a large group of preimplantation embryos. The large embryo group (red arrows) remained relatively intact and stable over 2 h (Video S6).

(B) Separation of an individual embryo from a large embryo group (Video S7).

(C) Grouping of an individual embryo with a three-embryo group (Video S8).

(D) Embryo trajectories over the grouping event.

(E) Speed of the individual embryo and embryo groups over the grouping event.

(F) Linear regressions of the speed of embryo groups versus the number of embryos within the group showing that both the average and maximum speed of the group are dependent on the number of embryos. The more embryos in the group, the lower the speed of the group. The speed data represent the mean value from all embryos in the corresponding size of groups. Observations were made in three mice. Scale bars: 200 μm.

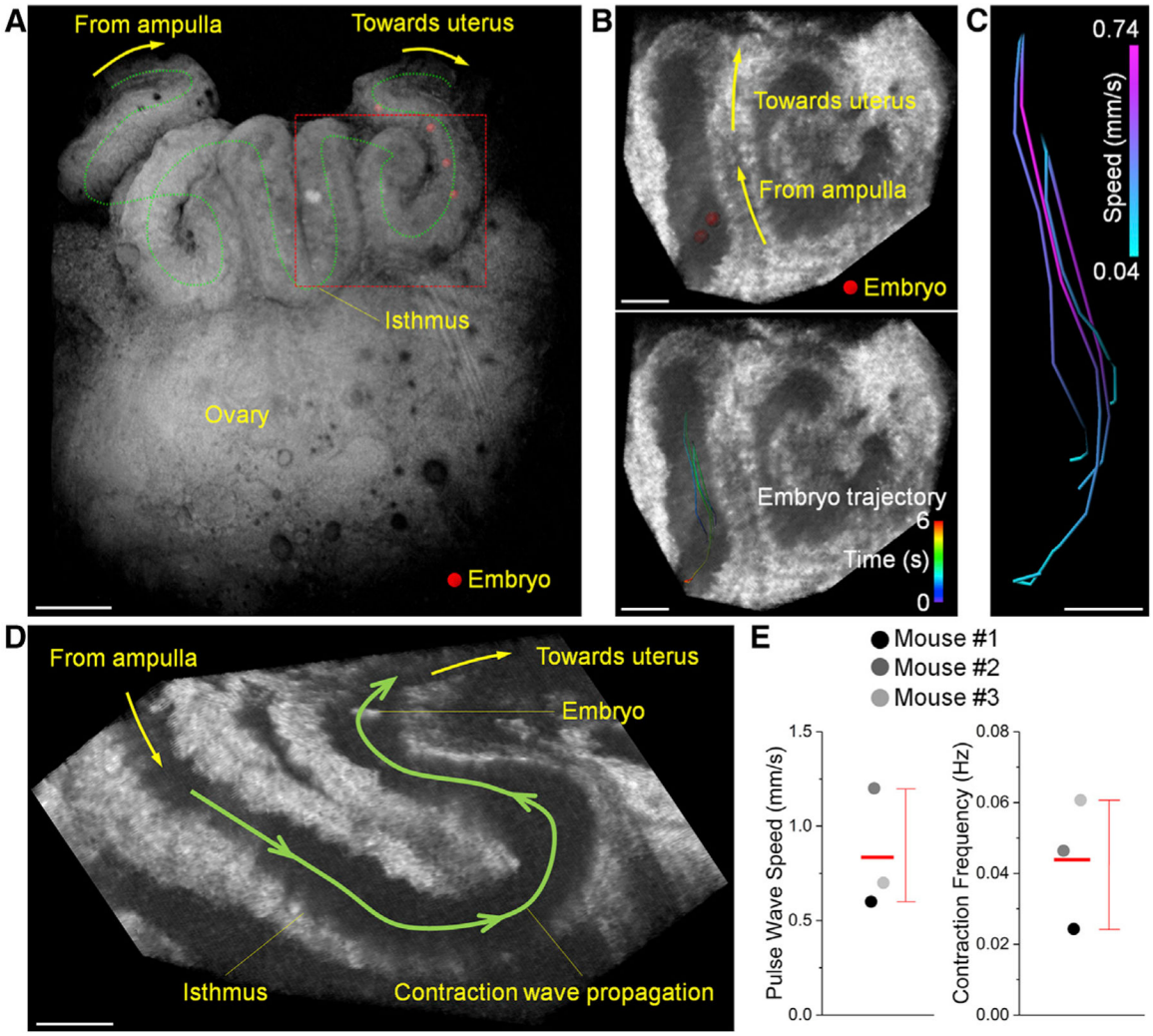

Figure 5. Bi-directional, fast, long-distance movements of preimplantation embryos with peristaltic luminal contraction waves in the isthmus

(A) Volumetric OCT view shows the location of preimplantation embryos in the isthmus.

(B) Cross-section through the volumetric time lapse with representative embryo trajectories demonstrates forward and backward movements of embryos (Video S9). The bi-directional movements of preimplantation embryos were observed in two mice.

(C) Trajectories color-coded with the movement speed from two embryos.

(D) Peristaltic luminal contraction wave propagation in the isthmus (Video S10).

(E) Average wave speed and contraction frequency in the isthmus. Red line: mean; whiskers: range. Scale bars: 500 μm (A); 200 μm (B and D); 100 μm (C).

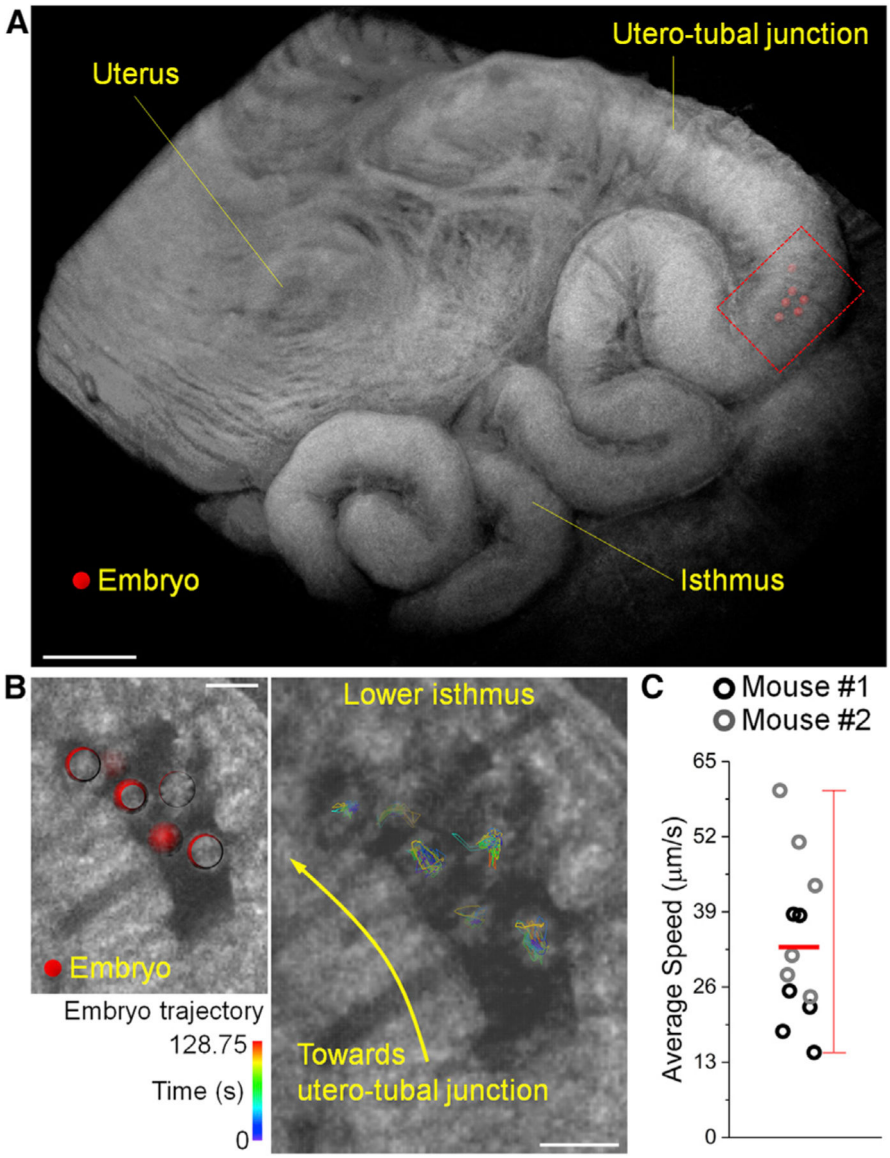

Figure 6. Localized oscillations of preimplantation embryos in the lower isthmus at the entrance to the utero-tubal junction

(A) Volumetric OCT view shows the location of preimplantation embryos in the lower isthmus close to the utero-tubal junction.

(B) Segmentation and tracking of embryos revealed localized oscillating movements (Video S11).

(C) The average speed of localized embryo oscillations. Red line: mean; whiskers: range. Scale bars: 500 μm (A); 100 μm (B).

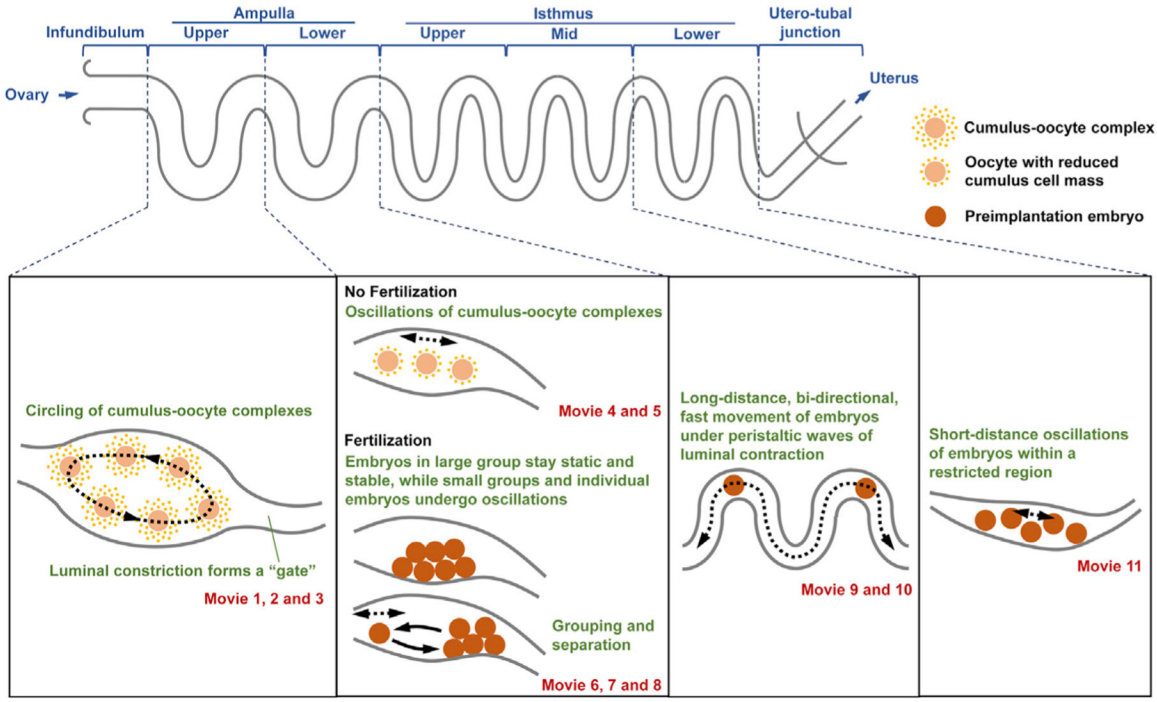

Figure 7.
Summary of observed oocyte/embryo dynamics in different regions of the oviduct

KEY RESOURCES TABLE

REAGENT or RESOURCE	SOURCE	IDENTIFIER
Experimental models: organisms/strains		
Mouse (wild-type, CD-1)	Charles River Laboratories	Strain code: 022
Software and algorithms		
Imaris	Oxford Instruments	https://imaris.oxinst.com/
ImageJ	NIH	https://imagej.nih.gov/ij/
Other		
Drawing of the dorsal intravital window with detailed dimensions	Wang et al., 2018	jbio201700316-sup-0004-FigureS1.docx
3D printer	Formlabs	Form 2
Resin	Formlabs	Grey resin